In situ MÖSSBAUER STUDY OF THE PASSIVE LAYER FORMED ON THE IRON ANODE IN ALKALINE ELECTROLYTE

Karel BOUZEK[a,*] and Martin NEJEZCHLEBA[b,c]

[a] *Department of Inorganic Technology, Prague Institute of Chemical Technology, Technická 5, 166 28 Prague 6, Czech Republic; e-mail: bouzekk@vscht.cz*

[b] *Institute of Inorganic Chemistry, Academy of Sciences of the Czech Republic, Peléova 26, 160 00 Prague 6, Czech Republic*

[c] *Joint Laboratory of Mössbauer Spectroscopy, Faculty of Mathematics and Physics, Charles University, V Holešovičkách 2, 180 00 Prague 8, Czech Republic; e-mail: martin.nejezchleba@mff.cuni.cz*

Received August 18, 1998
Accepted June 16, 1999

In situ Mössbauer spectra of the iron electrode at anodic potential were measured in sodium hydroxide solution over a wide range of concentrations (0.1–14 mol l^{-1}). It was found that the *in situ* Mössbauer spectra exhibit generally one sextet and one doublet corresponding to the oxide layer on the anode surface. Parameters of these spectra show only minor variations within the electrolyte concentration range of 0.1–7 M NaOH. A pronounced change in the spectra was observed in 14 M NaOH. The major processes taking place in the anode surface layer are based on the break-down of protective properties of the passive layer, incipient intense metal dissolution and subsequent oxidation. Important differences were also found between *in situ* and *ex situ* spectra measurements.

Key words: Mössbauer spectroscopy; Corrosion resistivity; Composition; Hydroxide concentration; Cathodic activation; Electrochemistry; Iron.

Mössbauer spectroscopy is a well established experimental method allowing the *in situ* characterization of iron compounds which appear on the surface of iron electrode when anodic potentials are applied[1,2]. That is, why the Mössbauer spectroscopy is used, from the electrochemical point of view, mostly in corrosion engineering to provide a better understanding of the passive layers, their formation and properties. For these purposes, the Mössbauer spectroscopy experiments were performed at the open circuit and/or anodic potentials in borate[3–5] or in solutions simulating acid rain[6–11]. The influence of chlorides in the electrolyte solution was also studied[12,13].

The iron passive layer exhibits itself in the Mössbauer spectrum by a doublet. It is interpreted as an amorphous ferric oxide[4], γ-FeOOH (refs[6–9,12]),

α-FeOOH or γ-Fe_2O_3 (ref.[12]) and β-FeOOH (refs[12,13]) depending on the experimental conditions.

The behaviour of iron and its compounds in highly concentrated alkali metal hydroxide solutions was also studied[14–18]. The Mössbauer spectroscopy helps to understand various processes, such as electrocatalytic oxygen evolution[14], charging and discharging processes in alkaline batteries[15] and iron chemistry in concentrated alkali metal hydroxide solutions[16–18].

Conditions relatively close to the present study were employed by Geronov *et al.*[19], who used Mössbauer spectroscopy to characterize the products formed on iron electrode in alkaline solutions during cyclic voltammetric meassurements.

The Mössbauer spectra of sodium ferrates were measured by Kopelev *et al.*[20] The *ex situ* studied samples were prepared by oxidation of Fe_2O_3 by Na_2O_2 at elevated temperature.

Relatively wide range of problems was studied by Mössbauer spectroscopy, but it does not include the *in situ* identification of the oxide layer formed on the iron anode in strongly alkaline electrolytes. This problem however, was already investigated by other methods, mainly using the *ex situ* instrumentation[21,22].

It was shown in the previous work[23] that with increasing hydroxide concentration and/or the electrolyte temperature the current density in region of metal passivity increases. This observation is in agreement with the theory proposed by Zou and Chin[24] who considered the reaction of the passive layer with the hydroxide anion. This indicates the relation between changes in the passive-layer properties and increasing electrolyte alkalinity. At the same time, it was found that during iron anode oxidation to ferrate(VI) in concentrated hydroxide solutions, the electrode activity in the transpassive potential region is gradually lowered[25–27], possibly due to the anode surface deactivation by formed oxide layer[27].

The aim of this paper is to contribute to a deeper understanding of the problem of interaction between hydroxide ions and oxide layer on the iron surface in the transpassive potential region.

EXPERIMENTAL

Chemicals

The sodium hydroxide (Spolana, Prague, Czech Republic) contained according to certificate the following maximum concentrations of impurities (in wt.%): Cl 0.008, Ag 0.002, Fe

0.002, Al 0.002, PO_4^{3-} 0.005, and Ca^{2+} 0.001. Concentrations of solutions ranged from 0.1 to 14 mol l^{-1}.

The iron foil 50 μm thick was used as a working electrode. The commercial steel electrode material has the following composition (in wt.%): C 0.68, Mn 0.57, Si 0.19, P 0.025, S 0.025, Co 0.10, Ni 0.02, Cu 0.06, Mo 0.002, Ti 0.003 and Sn 0.006. Concentrations of all other elements were lower than 0.001%. Nickel plates were used as counter electrodes.

Apparatus

The spectra were measured using standard transmission Fe^{57} Mössbauer spectrometer connected to an IBM PC *via* a multichanell card EG&G MCS+. Radiation source Co^{57} in a chromium matrix was used. All isomer shift values given in the text are referred to α-Fe.

The Wenking Potentiostat 70 HC 3 in galvanostatic regime connected to the electrochemical cell was used for *in situ* experiments (Fig. 1). The clean working electrode placed in the upper part of the cell was electrochemically oxidized at a current density of 20 mA cm^{-2}. After 30 min of electrolysis, the applied current was lowered to 10 mA and the electrode was moved to the bottom of the cell where the Mössbauer spectra were taken. The thickness of the electrolyte on each electrode side was 2.3 mm. The time necessary for measuring spectra with satisfactory quality varied from 4 to 14 days for *in situ* experiments depending on the electrolyte concentration. An *ex situ* arrangement reduced the meassurement period to 24 h. All experiments were performed at the room temperature if not otherwise indicated.

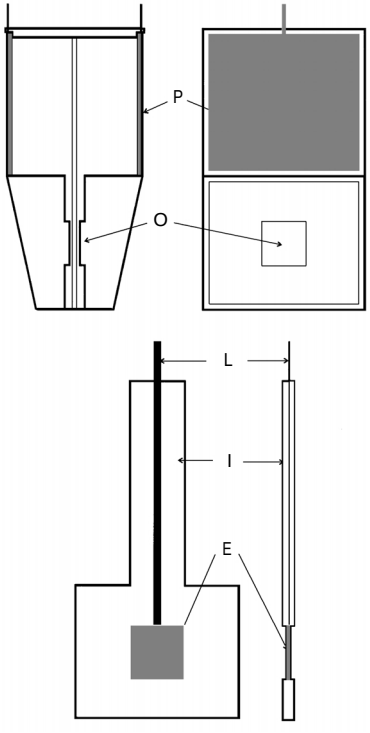

FIG. 1
Electrochemical cell used in *in situ* experiments; P cathode, O poly(methyl methacrylate) window, I anode insulation frame, L anode current lead, E anode

THEORETICAL

Mathematical Model

Low thickness of the electrolyte layer at the sample electrode surface was kept because of strong γ-ray beam attenuation in the electrolyte layer, especially at higher electrolyte concentrations. Since the cathodes are located in the upper part of the cell (Fig. 1), our arrangement represents a compromise between requirements of an even local current density distribution and the electrolyte thickness which allows spectra to be taken in a reasonable time period. Therefore, a three-dimensional mathematical model of the electrochemical cell was developed to optimize the cell construction and the anode position.

Description

The local current density distribution was calculated in a three-dimensional model of the experimental cell. The schematic cross-section of the model cell is shown in Fig. 2. Due to the symmetry of the cell in the plane $x = lx_1 + lx_4$, only the half-cell including the cathode and one side of the anode was considered to reduce the time of calculation. Potential drop on the electrode ohmic resistance was neglected.

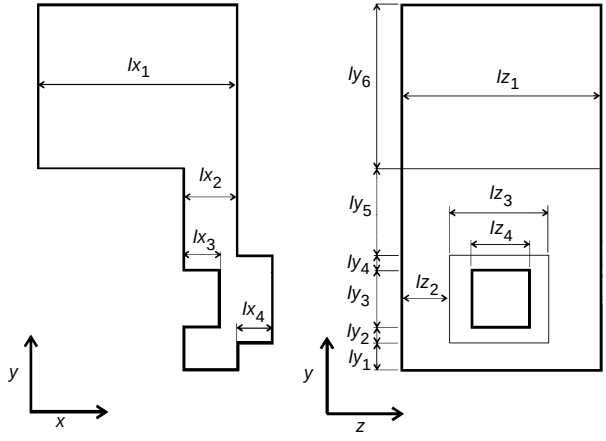

FIG. 2
Schematic cross-section of the cell used for calculation of local current densities. Dimensions (in cm): lx_1 = 2.65, lx_2 = 0.25, lx_3 = 0.2, lx_4 = 0.18, ly_1 = 1.45, ly_2 = 0.32, ly_3 = 2.50, ly_4 = 0.18, ly_5 = 2.4, ly_6 = 7.50 cathode, lz_1 = 6.00 cathode, lz_2 = 1.50, lz_3 = 3.00 anode, lz_4 = 2.60

Equation for the Potential Distribution

The distribution of the potential can be obtained by solving Eq. (*1*).

$$\nabla(-\kappa\nabla\varphi) = 0 \qquad (1)$$

For systems with uniform electrolyte conductivity, this equation is simplified to the Laplace equation

$$\nabla^2\varphi = 0\,. \qquad (2)$$

Boundary Conditions

Since the secondary current distribution was calculated, the Tafel equation with respective coefficients was used as a boundary condition on the electrode surface.

$$E = a + b\ln|j| \qquad (3)$$

For the cathode surface the following constants of the Tafel equation were used at 0.1, 1, 7 and 14 M NaOH: a = –1.003 V, b = –0.063 V; a = –1.105 V, b = –0.061 V; a = –1.150 V, b = –0.045 V; a = –1.128 V, b = –0.059 V.

For the anode surface voltammetric curves were measured by the method described in ref.[28]. The following Tafel equation constants were found for 0.1, 1, 7 and 14 M NaOH: a = 0.765 V, b = 0.026 V; a = 0.727 V, b = 0.019 V; a = 0.659 V, b = 0.027 V; a = 0.582 V, b = 0.036 V.

At the cell walls and at the electrolyte surface a zero potential gradient was considered:

$$\frac{\partial\varphi}{\partial n} = 0\,, \qquad (4)$$

where n is the direction normal to the cell wall and electrolyte surface.

Equation (*2*) was solved by the conservative scheme method[29]. The boundary conditions described by Eqs (*3*) and (*4*) were used for the calculation.

Mathematical Model Results

The final dimensions of the cell are indicated in Fig. 2. Calculated local values of the anodic current density are shown in Fig. 3 for 14 M NaOH. It is obvious that even for high current density variations at the anode surface, the region studied exhibited regular current density distribution with only minor variations. Average current densities in the observed range were 1.41, 1.45, 1.49 and 1.71 A m^{-2} for 0.1, 1, 7 and 14 M NaOH. The potentials of the electrode in the monitored area had the values of: 774 , 734, 670 and 601 mV *vs* HgO/Hg reference in 14 M NaOH.

RESULTS

The optimum velocity range for *in situ* Mössbauer spectroscopy was estimated, using 14 M NaOH solution, as ±8 mm s^{-1}. All the experiments at the room temperature were therefore performed using this velocity range. The best fit of the experimentally obtained spectrum was attained by four subspectra. Three of them were identified as sextets, one as a doublet. The first two sextets correspond to the iron matrix and to the surface layer of iron with destroyed crystalline structure, possibly amorphous. The origin of this layer is associated with the metal dissolution causing the destruction of

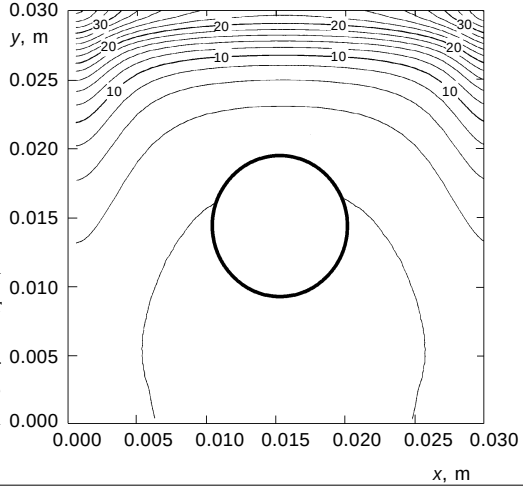

FIG. 3
Calculated local current density distribution isolines on the anode surface for 14 M NaOH solution: total current 10 mA. Numbers in the graph indicate the current density (in A m^{-2}). The circle in the centre of the figure indicates the area examined

the crystalline structure and, at the same time, with gas evolution proceeding in parallel at the anode surface. The contribution of the oxide film to the total spectrum is one doublet and one sextet. The results of *in situ* experiments with iron electrode maintained at anodic potential and spectra corresponding to 0.1, 1, 7 and 14 M NaOH solutions are summarized in Fig. 4, where v represents the velocity. The values of the isomer shift with respect to α-Fe standard as well as other important subspectra parameters are summarized in Table I. The high γ-ray beam attenuation in the case of the highest studied electrolyte concentration, 14 mol l^{-1}, causes a lower Mössbauer effect compared to 0.1 M NaOH solution. Therefore, the time for recording the spectra with satisfactory statistical certainty is 14 days for 14 M NaOH. This time was reduced to 4 days for 0.1 M NaOH.

The application of sufficiently high cathodic potential on the iron electrode in alkaline electrolyte was found to cause an activation of its surface for anodic dissolution[28]. This behaviour was explained by the formation of fine, very reactive metallic iron particles. An experimental verification was performed on the electrode by alternation of anodic potential applied for 14 days with cathodic potential. The oxide layer built up on the iron anode

TABLE I

Parameters of the subspectra corresponding to the iron oxides and hydroxides in the oxide layer covering the anodically polarized iron electrode in NaOH solution (*in situ* experiments). ISO, isomer shift *vs* α-Fe; QUA, quadrupole splitting; DEP, absorption line intensity; WID absorption line width; HMF, hyperfine magnetic field; DHMF, magnetic field distribution width; PA, subspectrum relative area

Subspectrum	Electrolyte concentration mol l^{-3}	ISO mm s^{-1}	QUA mm s^{-1}	DEP	WID mm s^{-1}	HMF T	DHMF T	PA %
Doublet	0.1	–0.01	1.70	0.0046	0.411	–	–	6.2
	1	0.04	1.71	0.0030	0.328	–	–	5.6
	7	0.0	1.72	0.0031	0.441	–	–	5.9
	14	0.31	0.87	0.0100	0.858	–	–	16.7
Sextet	0.1	0.21	0.04	0.0088	0.245	17.47	5.72	11.9
	1	0.17	–0.03	0.0064	0.239	17.21	6.24	12.1
	7	0.16	–0.05	0.0059	0.228	17.12	7.15	11.2
	14	0.39	–0.05	0.0049	0.261	16.25	6.83	8.2

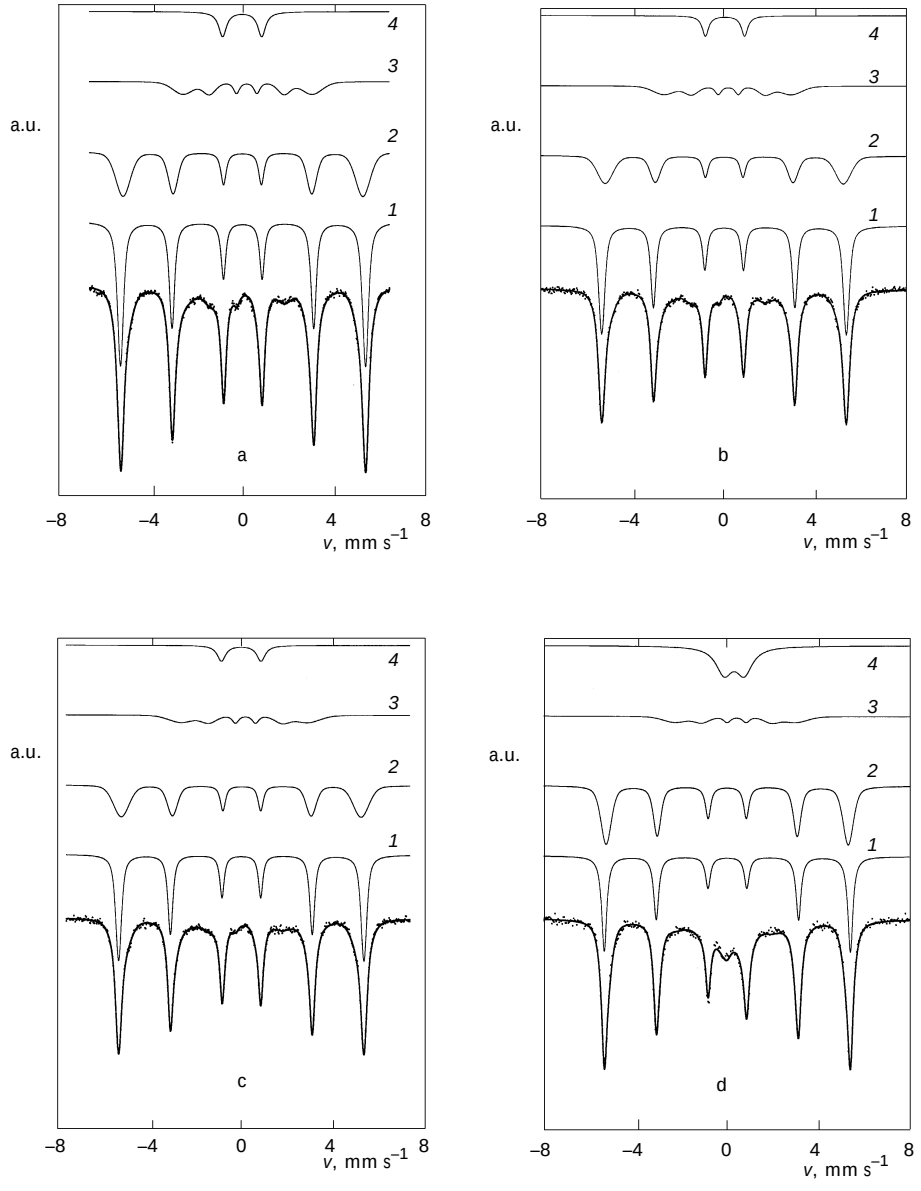

FIG. 4

In situ Mössbauer spectra of iron foil anodically polarized by the total current 10 mA, concentration of NaOH in electrolyte (in mol l^{-1}): a 0.1, b 1, c 7, d 14; ● experimental points, — fit of the experimental points, — individual subspectra; *1* bulk electrode material, *2* surface layer with damaged structure, *3* and *4* oxide layer; *v* represents the velocity

during its polarization was completely removed and/or reduced in subsequent application of cathodic potential. This is documented by Fig. 5. The doublet found in the spectrum when anodic potential was applied virtually disappeared. This indicates that the term "removed" is in this case more appropriate than "reduced". In 14 M NaOH the oxide layer consists of two clearly separated sublayers. The outer one is apparently thicker with a very low adhesion to the electrode surface. On many locations it is lost from the surface of an underlying material and can be easily removed just by touche. Plastic tool is preferred to avoid damaging underlying electrode material. Applying sufficiently high cathodic potential, the outer part of the oxide layer is removed from the surface by evolved hydrogen bubbles. This result indicates that the inner part of the oxide layer, which is (unlike the outer) very thin and has good adhesion to the electrode surface, corresponds to the sextet subspectrum. This will be discussed in more detail later on. The intensity and parameters of the sextet changed substantially during applying cathodic potential. Its isomer shift decreased to –0.03 mm s^{-1} and quadrupole splitting to –0.31 mm s^{-1}. The width of the absorption lines and the hyperfine magnetic field remained virtually the same as with the anodic potential applied, but hyperfine magnetic field distribution increased to a value of 21.46 T.

After the experiment in 14 M NaOH, the sample was washed in distilled water and dried in air at the room temperature. The Mössbauer spectrum was taken 1 h and then 30 days after the electrode was washed. The

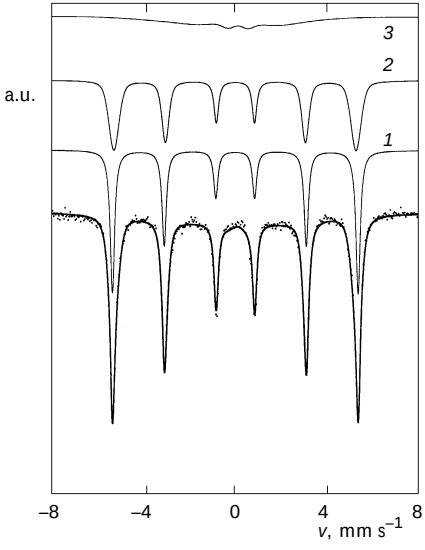

FIG. 5

In situ Mössbauer spectra of iron foil cathodically polarized by the total current 20 mA; the studied electrode was polarized prior to the cathodic polarization for two weeks anodically at 10 mA. ● Experimental point, ▬ fit of the experimental points, — individual subspectra; *1* bulk electrode material, *2* surface layer with damaged structure, *3* reduced oxide layer (iron particles)

Mössbauer spectrum measured after 30 days of drying is shown in Fig. 6. The best fit was found for four sextets and one doublet. The first three sextets were identified to belong to the bulk iron electrode and to the surface

TABLE II

Parameters of the subspectra corresponding to the iron oxides and hydroxides in the oxide layer covering the iron electrode previously anodicaly polarized for two weeks in 14 M NaOH solution. For abreviations, see Table I. Experiment description: *in situ*, *in situ* experiment with anodically polarized electrode; *ex situ* I, *ex situ* experiment performed with the electrode from the previous experiment, after washing in distilled water and drying in air for 1 h; *ex situ* II, *ex situ* experiment performed with the electrode from *ex situ* I after 30 days drying in air

Subspectrum	Electrolyte concentration mol l^{-3}	ISO mm s^{-1}	QUA mm s^{-1}	DEP	WID mm s^{-1}	HMF T	DHMF T	PA %
Doublet	*in situ*	0.31	0.87	0.0100	0.858	–	–	16.7
	ex situ I	0.31	0.77	0.0776	0.844	–	–	22.7
	ex situ II	0.35	0.70	0.0501	0.546			17.8
Sextet	*in situ*	0.39	–0.05	0.0049	0.261	16.25	6.83	8.2
	ex situ I	0.39	0.05	0.0289	0.254	15.56	7.32	8.4
	ex situ II	0.12	–0.08	0.0487	0.211	13.68	19.07	17.3

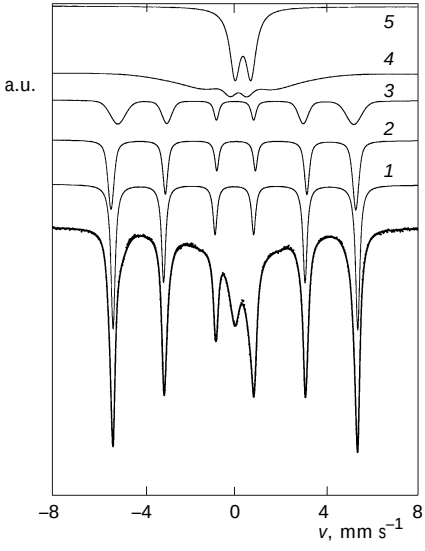

FIG. 6

Ex situ Mössbauer spectrum of iron foil preliminary treated by anodic polarization at 10 mA in 14 M NaOH for two weeks, washed in distilled water and dried in the air. ● Experimental point, ▬ fit of the experimental points, — individual subspectra; *1* bulk electrode material, *2* and *3* surface layer with damaged structure, *4* and *5* oxide layer

layer with damaged crystalline structure. One sextet and one doublet correspond to the oxide layer. The values of parameters of both *ex situ* and *in situ* collected spectra are compared in Table II. After the spectra were measured, the outer nonadhesive layer was mechanically removed using plastic sharp tool as discussed previously and studied separately. Its Mössbauer spectrum

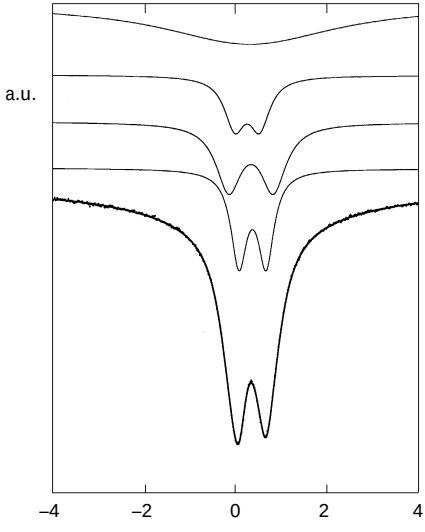

FIG. 7

Ex situ Mössbauer spectrum of the outer, nonadhesive oxide layer removed mechanically from the sample shown in Fig. 6. ● Experimental point, ▬ fit of the experimental points, — individual subspectra

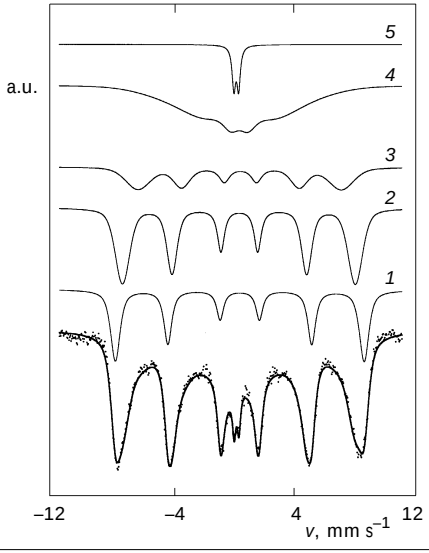

FIG. 8

Ex situ Mössbauer spectrum of the outer, nonadhesive oxide layer removed mechanically from the sample shown in Fig. 6 at the temperature of the liquid nitrogen. ● Experimental point, ▬ fit of the experimental points, — individual subspectra; *1* Fe_3O_4, *4* amorphous phase, *2*, *3* and *5* iron oxide phases

shown in Fig. 7 confirms the expectation that outer nonadhesive part of the oxidic layer is responsible for the appearance of doublet in the *in situ* spectrum of iron electrode at anodic potentials. The doublet was best fitted by four subspectra. Afterwards a spectrum of this sample was measured at the temperature of 77 K (Fig. 8).

As a complementary method an X-ray diffraction was used for the identification of the outer oxide layer. The X-ray diffraction pattern measured on oxide powder is shown in Fig. 9.

DISCUSSION

The results shown in Table I document clearly the important influence of the NaOH concentration on processes taking place on the iron surface. We can clearly see that within the concentration region from 0.1 to 7 M NaOH changes in Mössbauer spectra are almost negligible. Also the intensity of absorption lines corresponding to the oxide layers is relatively low. But important changes in spectrum parameters appear in 14 M NaOH which was the highest studied concentration. This is in a good agreement with the visual observation. Whereas at lower NaOH concentrations the anode surface does not show any visible surface oxide layer formation, at the highest NaOH concentration, the anode material was apparently dissolved and its

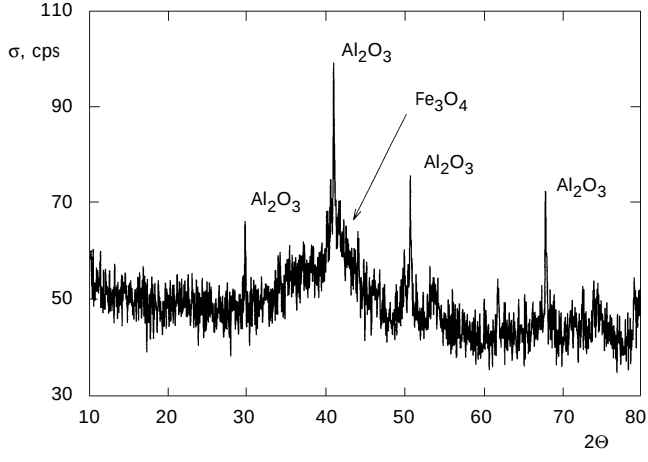

FIG. 9
X-Ray diffraction patterns of the outer, nonadhesive oxide layer removed mechanically from the sample shown in Fig. 6; σ is the intensity in counts per second (cps)

surface was covered by a reddish-brown, thick oxide layer. The thickness of the oxide layer was not estimated in these experiments.

The isomer shift of the sextet observed at concentrations below 7 M NaOH indicates iron in its oxidized state. Nevertheless, the other parameters indicate more likely an amorphous metallic iron. We have to deal with a problem of very broad distribution of the absorption lines and, at the same time, their relatively low intensity. This makes the identification of the origin of these subspectra, without any additional experimental techniques, rather difficult. A probable explanation can be found in a very thin oxide layer at the metal surface and formation of quasi-intermediate phase between metal and the outer oxide layer. From the parameters found, we may assign this subspectrum to species with the composition close to goethite (α-FeOOH) or magnetite (Fe_3O_4).

It should be remembered that analysis of this kind has to be taken carefully. It is well known that the passive film on the iron surface does not exhibit any regular crystalline structure[2,4]. Also, compounds present in passive layer are only rarely included in a stoichiometric form. Moreover, they are hydrated to a significant extent influencing thus the Mössbauer spectra parameters. Therefore, proposed iron oxides and oxo-hydroxides are the closest to the obtained Mössbauer spectra and should be taken as closely describing the real situation at the iron surface.

The increase in the isomer shift with rising electrolyte concentration above 7 mol l^{-1} may indicate either change in the oxidation number of iron in oxide layer or, more likely, changes in the ratio between di- and trivalent iron atoms within the layer. We also observe a slight decrease in the hyperfine magnetic field. This points to the increasing degree of disorder in the layer structure. The last important change is manifested by a decrease in the relative subspectrum area corresponding to the sextet. It should be noted, that in the case of the highest concentration of NaOH the uncertainty of parameters remains an important factor.

Quadrupole splitting of the doublet observed in all spectra indicates an oxide layer. Unfortunately, other parameters do not make it possible to identify directly its nature. For the electrolyte concentrations up to 7 M NaOH the oxide film is probably very thin which affects the absorption lines width determined not only by the oxide structure but also by its thickness. Another parameter influenced by the thickness of the oxide film is the quadrupole splitting. Its value may be increased substantially for thin layers of studied material.

At the highest NaOH concentration, the parameters of the doublet changed significantly. While the isomer shift increase points again to the

change in iron oxidation states or their ratio, the decrease in the quadrupole splitting can be explained by the change in the composition, the increase in the layer thickness or changes in the ratio between two different layers. The first of these structures is represented, as discussed above, by sextet and the second by doublet. An increase in the doublet intensity may than cause the evaluated decrease in the quadrupole splitting.

The increase in absorption lines width observed for the doublet indicates, that this part of the oxide layer is highly porous and its hydration degree remarkably increased.

Thus, in the concentration range up to 7 M NaOH, the inner oxide layer represented by the sextet, offers relatively good protection to the bulk material and virtually no dissolution was observed. This corresponds to the very low intensity of the doublet. If the electrolyte concentration exceeds 7 mol l^{-1}, the inner oxide layer breaks down and intensive material oxidation followed by subsequent dissolution takes place. This process is associated with a significant increase of doublet intensity and, at the same time, with a decrease in the intensity of the inner layer subspectrum. The outer layer becomes thick and judging from the broad absorption line, disordered and porous. The increase in the isomer shift may be caused by an increased concentration of trivalent iron in the oxide layer.

This observation is in agreement with previous studies on ferrate(VI) formation[26,27]. The iron was found to dissolve most intensively in the concentration range of 14–16 M NaOH. In 5 M NaOH the current efficiency decreased rapidly to 10% of its maximum value, apparently due to decreasing OH^- ion activity which slowed down the kinetics of its reaction with surface oxide layer. Also, the presence of thick, porous oxide layer on the anode surface is considered to have positive influence to ferrate(VI) formation[28]. The importance of the electrolyte concentration is confirmed by the above Mössbauer spectroscopy results.

Although the Mössbauer spectra for alkaline solutions resemble very close by previously published results for borate buffer solutions[3–5], parameters of the doublet found in previous studies differ from those for highly alkaline electrolyte. For the first time, the sextet corresponding to oxidized iron in the surface layer was observed as a part of the passive layer. On the other hand, it was already observed in charging–discharging of the iron electrode in an alkaline electrolyte[19].

It was generally accepted that drying causes mostly irreversible changes in the structure and composition of passive layer. Therefore, the *in situ* techniques are recommended for the study of passive-layer composition and properties[2].

From the results obtained in this study, it is apparent that the layer corresponding to the doublet in the Mössbauer spectrum does not undergo important changes during drying and exposure to the air. Only the width of the absorption lines decreases after 30 days of exposure to the atmosphere. This indicates agglomeration of fine particles in the oxide layer and formation of phase with more regular structure.

The parameters of the sextet show more pronounced changes. First of all, an important decrease in the isomer shift, together with an increase of the relative spectrum area indicates a continuous oxidation of bulk iron material with oxygen, enabled by the water included in the porous structure of the oxide layer (see Table II). The continuous oxidation may cause either an increase in divalent iron concentration due to the continuous bulk material dissolution or changes in its structure.

The time decrease of the layer hydration results in structural changes of the oxide layer. The process is responsible for the decrease in hyperfine magnetic field and increase in magnetic field distribution width (see Table II).

The *ex situ* Mössbauer spectrum of mechanically removed, outer nonadhesive part of the oxide layer is presented in Fig. 7. The doublet observed in the previous spectra corresponds to the outer part of the passive layer with poor protecting properties. This would confirm that in accord with the general theory of duplex possive-layer structure[21,31–34], the inner protecting layer is represented by the sextet and the outer, nonprotective part of the oxide layer by the doublet. The parameters of the doublet calculated using an expanded *ex situ* spectrum indicate the composition of this layer to be close to α-Fe_2O_3 or Fe_3O_4 again. As shown in Fig. 7, the spectrum of the outer part of the oxide layer consists of four subspectra. This fact can be explained by the proposed presence of the iron oxide in more phases differing in the degree of their crystalline structure disorder, by the presence of admixtures of iron ions or oxides in lower oxidation stages or by the presence of an additional oxide phase which was not yet identified. Mössbauer spectrum of the mechanically removed outer layer at the temperature of 77 K is best fitted by 5 subspectra. Subspectrum *1* indicates the presence of Fe_3O_4. Subspectrum *4* belongs to practically amorphous phase. Remaining subspectra *2*, *3* and *5* belong to the iron oxides. We may consider they correspond to more phases of Fe_3O_4 differing in the degree of their disorder or to another not yet identified iron oxide. Also the X-ray diffraction pattern shown in Fig. 9 indicates the presence of Fe_3O_4 in the sample. Four strong reflection lines apparent on the pattern correspond to the corundum (α-Al_2O_3) added to the sample artificially prior the Mössbauer experiment to increase its volume to a required level. Comparison of these results

proves the identification of the outer layer as Fe_3O_4. The main difference between the external and internal layers is in an extent of their structure disorder. The spectrum of the outer layer indicates, compared to internal one, lower compactness and more disordered structure, formed possibly by small particles. The X-ray broad reflection peak indicates the presence of Fe_3O_4 particles with the size below 50 nm.

The results obtained for cathodicaly polarised iron electrode, shown in Fig. 5, confirm that the electrode surface is activated during electrochemical reduction period. The disappearance of the doublet from the Mössbauer spectrum indicates virtually complete removal of the outer oxide layer by the electrochemical reduction. Moreover, the change of sextet parameters indicates that inner, protecting layer, was completely reduced to amorphous metallic iron, probably in the form of very fine particles. This is also in an agreement with previously proposed mechanism[28].

CONCLUSION

Two subspectra corresponding to the oxide film formed on the iron surface during its anodic polarisation in NaOH solution were identified by *in situ* Mössbauer spectroscopy. First of them was found to correspond to the inner layer located on the metal surface with good protective properties. The other can be assigned to the oxide located on the interface between the electrolyte and inner layer. It shows high porosity and poor protection of bulk metal against dissolution.

The Mössbauer spectroscopy has confirmed that intensive anodic iron dissolution and oxidation to ferrate(VI) is promoted by an increase in NaOH concentration. The reason is the breakdown of the inner oxide layer indicated by changes in composition and properties of both parts of oxide layer.

Changes in the surface oxide layer caused by drying in *ex situ* experiments set the validity limits of results obtained by above mentioned experimental techniques, especially in the case of inner protective oxide layer.

We had confirmed the activation of iron surface for oxidative dissolution by the application of preceding electrochemical reduction period.

Our thanks are due to the Joint SuperComputing Center ČVUT–VŠCHT–IBM, Prague for providing necessary computing facilities and to Dr J. Maixner for performing X-ray diffraction experiment.

REFERENCES

1. Varma R., Selman J. R.: *Techniques for Characterisation of Electrodes and Electrochemical Processes*. Wiley, New York 1991.
2. Abruna H. D.: *Electrochemical Interfaces: Modern Techniques for In situ Interface Characterisation*. VCH Publishers, New York 1991.
3. O'Grady W. E., Bockris J. O'M.: *Surf. Sci.* **1977**, *66*, 581.
4. O'Grady W. E.: *J. Electrochem. Soc.* **1980**, *127*, 555.
5. Eldridge J., Hoffman R. W.: *J. Electrochem. Soc.* **1989**, *136*, 955.
6. Kuzmann E., Varsányi M., Vértes A., Meisel W.: *Electrochim. Acta* **1991**, *36*, 911.
7. Lakatos-Varsányi M., Vertés C., Vertés A., Kiss L., Meisel W., Griesbach P., Gütlich P.: *J. Electrochem. Soc.* **1992**, *139*, 1301.
8. Vertés C., Lakatos-Varsányi M., Meisel W., Vértes A., Gütlich P., Kiss L.: *Electrochim. Acta* **1993**, *38*, 253.
9. Vértes C., Varsányi M. L., Vertés A., Meisel W., Gütlich P.: *Electrochim. Acta* **1993**, *38*, 2253.
10. Meisel W., Vértes C., Lakatos-Varsányi M.: *J. Radioanal. Nucl. Chem.* **1995**, *190*, 289.
11. Vértes C., Lakatos-Varsányi M., Vértes A., Meisel W., Horway A.: *ACH-Models Chem.* **1995**, *132*, 597.
12. Maeda Y., Matsuo Y., Sugihara S., Momoshima N., Takashima Y.: *Corros. Sci.* **1992**, *33*, 1557.
13. Waanders F. B., Vorster S. W.: *Hyperfine Interact.* **1994**, *92*, 1027.
14. Kamnev A. A., Ezhov B. B., Rusanov V., Angelov V.: *Electrochim. Acta* **1992**, *37*, 469.
15. Guerlou-Demourgues L., Fournes L., Delmas C.: *J. Electrochem. Soc.* **1996**, *143*, 3083.
16. Pritchard A. M., Mould B. T.: *Corros. Sci.* **1971**, *11*, 1.
17. Kamnev A. A., Ezhov B., Kopelev N. S., Kiselev Yu. M., Perfilyev Yu. D.: *Electrochim. Acta* **1991**, *36*, 1253.
18. Kamnev A. A., Perfilyev Yu. D., Angelov V.: *Electrochim. Acta* **1995**, *40*, 1005.
19. Geronov Y., Tomov T., Georgiev S.: *J. Appl. Electrochem.* **1975**, *5*, 351.
20. Kopelev N. S., Perfiliev Yu. D., Kiselev Yu. M.: *J. Radioanal. Nucl. Chem.* **1992**, *162*, 239.
21. Foley C. L., Kruger J., Brechtold C. J.: *J. Electrochem. Soc.* **1967**, *114*, 994.
22. Salkind A. J., Venuto C. J., Falk S. U.: *J. Electrochem. Soc.* **1964**, *111*, 493.
23. Bouzek K., Roušar I., Bergmann H., Hertwig K.: *J. Electroanal. Chem.* **1997**, *425*, 125.
24. Zou J.-Y., Chin D.-T.: *Electrochim. Acta* **1988**, *33*, 477.
25. Bouzek K., Roušar I.: *J. Appl. Electrochem.* **1996**, *26*, 919.
26. Bouzek K., Roušar I., Taylor M. A.: *J. Appl. Electrochem.* **1996**, *26*, 925.
27. Bouzek K., Roušar I.: *J. Appl. Electrochem.* **1997**, *27*, 679.
28. Bouzek K., Roušar I.: *J. Appl. Electrochem.* **1993**, *23*, 1317.
29. Roušar I., Kimla K., Micka K.: *Electrochemical Engineering I*. Elsevier, Amsterdam and Academia, Prague 1986.
30. Misawa T.: *Corros. Sci.* **1973**, *13*, 659.
31. Ogura K., Fujishima A., Honda K.: *J. Electrochem. Soc.* **1984**, *131*, 344.
32. Huang Z. Q., Ord J. L.: *J. Electrochem. Soc.* **1985**, *132*, 23.
33. Juanto S., Zerbino J. O., Miguez M. I., Vilche J. R., Arvia A. J.: *Electrochim. Acta* **1987**, *32*, 1743.
34. Albani O. A., Gassa L. M., Zerbino J. O., Vilche J. R., Arvia A. J.: *Electrochim. Acta* **1990**, *35*, 1437.